Thermoelectric Properties of Zintl Phase Compounds of Ca1−x Eu x Zn2Sb2 (0 ≤ x ≤ 1)

Article *in* Journal of Electronic Materials · December 2015

DOI: 10.1007/s11664-015-4303-6

5 authors, including:

Tessera Alemneh Wubieneh
Academia Sinica
3 PUBLICATIONS **0** CITATIONS
SEE PROFILE

Pai-Chun Wei
Academia Sinica
13 PUBLICATIONS **45** CITATIONS
SEE PROFILE

Journal of ELECTRONIC MATERIALS, Vol. 45, No. 3, 2016
DOI: 10.1007/s11664-015-4303-6

Thermoelectric Properties of Zintl Phase Compounds of $Ca_{1-x}Eu_xZn_2Sb_2$ ($0 \le x \le 1$)

TESSERA ALEMNEH WUBIENEH,[1,2,3,4] PAI-CHUN WEI,[3,6] CHIEN-CHIH YEH,[5] SZU-YUAN CHEN,[1,2,4] and YANG-YUAN CHEN[3,7]

1.—Department of Physics, National Central University, Taoyuan 32001, Taiwan. 2.—Molecular Science and Technology Program, Taiwan International Graduate Program, Academia Sinica, Taipei 10617, Taiwan. 3.—Institute of Physics, Academia Sinica, Taipei 11528, Taiwan. 4.—Institute of Atomic and Molecular Science, Academia Sinica, Taipei 10617, Taiwan. 5.—Center for Measurement Standards, Industrial Technology Research Institute, Hsinchu 300, Taiwan. 6.—e-mail: pcwei68@gmail.com. 7.—e-mail: cheny2@phys.sinica.edu.tw

p-Type $Ca_{1-x}Eu_xZn_2Sb_2$ ($0 \le x \le 1$) polycrystalline specimens were prepared by direct solid-state reaction of elements followed by appropriate annealing, grinding and spark plasma sintering for densification. The thermoelectric (TE) properties of Zintl phase $Ca_{1-x}Eu_xZn_2Sb_2$ were investigated by measuring resistivity, Seebeck coefficient and thermal conductivity from 300 K to 720 K. All Eu doped specimens show more than 50% decrease in electrical resistivity, while their Seebeck coefficient value only slightly decrease as compared to $CaZn_2Sb_2$. Furthermore, a reduction of thermal conductivity was achieved by the additional phonon scatterings of Eu dopants. The cationic substitution of rare earth element Eu in the Ca-site significantly increased the thermoelectric dimensionless figure of merit for all Europium substituted samples. Within this series, $EuZn_2Sb_2$ shows a good thermoelectric property with a maximum zT value of 0.98 at 720 K.

Key words: Zintl phase, thermoelectric, power factor, Seebeck coefficient

INTRODUCTION

The waste heat recovery using thermoelectric materials has attracted widespread research interest because of the significant improvement in the efficiency of TE materials for the past decades.[1–3] This gives the opportunity to provide a substantial amount of electrical power from exhausts, geothermal power, and other heat sources.[4,5] The efficiency of thermoelectric materials is determined by the dimensionless figure of merit, $zT = S^2T/\rho\kappa$, where ρ is the electrical resistivity, S is the Seebeck coefficient, T is the absolue temperature and κ is the thermal conductivity. Apparently, increasing the power factor and minimizing the thermal conductivity of TE materials are beneficial for obtaining higher zT. Currently, Zintl phase compounds have been considered as potential thermoelectric materials because of their unique characteristics of low thermal conductivity which comes from strong lattice anharmonicity, sufficient electronic conduction and high Seebeck coefficient.[6] Zintl phase compounds are generally small-bandgap semiconductors and the bonding can be described via the Zintl formalism as consisting of electropositive cations and covalently bonded network of complex anions or metalloids.[7] Fascinatingly, Zintl compounds enable various possibilities for chemical substitutions and structural modifications that allow the fine tune of individual transport parameters such as carrier concentration, mobility, effective mass and lattice thermal conductivity without affecting others. This provides the opportunity for optimizing their thermoelectric performance.

Many antimonide Zintl compounds such as $YbCd_{2-x}Mn_xSb_2$,[8] $Ca_xYb_{1-x}Zn_2Sb_2$,[9] $Yb_{14}MnSb_{11}$,[10] $Yb_{1-x}Ca_xCd_2Sb_2$,[11] $Ca_{11}GaSb$,[12] Sr_3AlSb_3,[13] $Sr_5Al_2Sb_6$,[14] and AZn_2Sb_2 (A = Sr, Ca, Yb, Eu)[15] have shown promising thermoelectric efficiency.

(Received July 20, 2015; accepted December 11, 2015; published online December 29, 2015)

Among them $CaZn_2Sb_2$ is a good candidate for thermoelectric material because it's cheap, non-toxic constituent elements and environmental-friendly. Moreover, $CaZn_2Sb_2$ is a semiconductor with band gap of about 0.26 eV.[16,17] As shown in Fig. 1, it crystallizes in the $CaAl_2Si_2$ structure-type and contains Zn–Sb anionic sheets which have mostly covalent character due to the similar electronegativity of Zn and Sb. The $(Zn_2Sb_2)^{2-}$ framework has good hole mobility due to its low polarity.[6] Herein, we demonstrate that the substitution of Eu for Ca sites in $Ca_{1-x}Eu_xZn_2Sb_2$ ($0 \le x \le 1$) is an excellent method to tune the thermoelectric transport property.

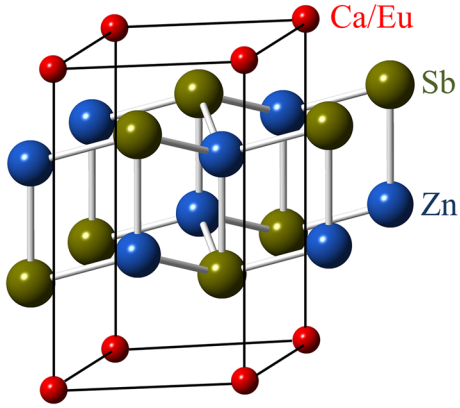

Fig. 1. The crystal structure of $Ca_{1-x}Eu_xZn_2Sb_2$ showing $(Zn_2Sb_2)^{2-}$ layers and Eu^{+2}, Ca^{+2} cations.

EXPERIMENTAL

Polycrystalline of $Ca_{1-x}Eu_xZn_2Sb_2$ ($0 \le x \le 1$) compounds were prepared by direct reactions of a mixture of properly weighed Eu (99.99%), Zn (99.9999%), Sb (99.99%) and Ca (99.95%). All materials are managed in a nitrogen-filled glove box with H_2O/O_2 levels below 1.0 ppm. The stoichiometric mixtures were loaded in a boron nitride crucible enclosed in fused-silica ampoules that were flame-sealed under dynamic vacuum. These assemblies were then held at 1000°C for 3 days and subsequently cooled to room temperature. The products were finely ground, pressed into pellets, and annealed at 800°C for 5 days. The annealed samples were then sintered by spark plasma sintering (SPS 2040) at 525°C for 15 min under a uniaxial pressure of 50 MPa in vacuum. The density of all the samples was measured by the Archimedes method and the densities of the measured samples were around ~96% of the theoretical value. X-ray diffraction was performed using PANalytical X'Pert PRO diffractometer operated at 45 kV and 40 mA, and Rietveld analysis was performed using HighScore Plus. The electrical conductivity and Seebeck coefficient were simultaneously measured using ZEM-3. The thermal conductivity (κ) was calculated from the measured thermal diffusivity (D), specific heat (c_p) and density (d) using the relationship $\kappa = Dc_pd$. The thermal diffusivity was measured by the laser flash diffusivity method using a Netzsch LFA 457 system, c_p was estimated by Dulong–Petit law and d was obtained using the Archimedes method. The Hall carrier concentration was measured using a physical property measurement system (Quantum design, USA) with magnetic field of ±2T.

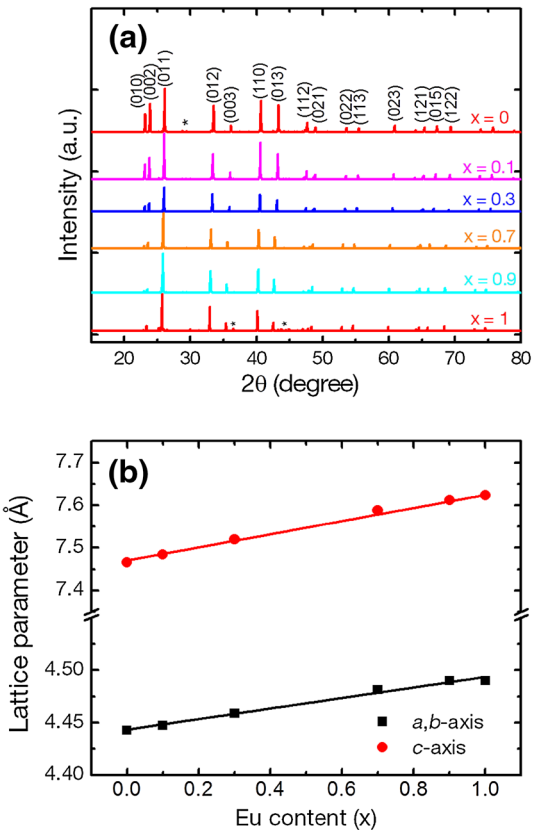

Fig. 2. (a) The XRD patterns for $Ca_{1-x}Eu_xZn_2Sb_2$ and the asterisks indicate the presence of impurity phases. (b) The calculated lattice parameters *a, b-* and *c*-axis as a function of Eu content.

RESULTS AND DISCUSSION

The x- ray diffraction (XRD) patters were taken to examine the phase purity of the samples. The XRD patterns for Eu-substituted $Ca_{1-x}Eu_xZn_2Sb_2$, ($0 \le x \le 1$) samples are shown in Fig. 2a. All of which are identified as a $CaAl_2Si_2$ structure. The scattering peaks were indexed to $CaZn_2Sb_2$ structure (reference code: 01-071-1815) and a trace amount of second phase was detected. The additional peaks seen in the XRD spectra are most likely due to small amounts of oxidation results during unavoidable exposure of the sample to air. This impurity phase may affect the transport property of the sample, but only to a negligible extent. The corresponding room temperature lattice parameters as a function of the Eu content are indicated in Fig. 2b. The lattice parameters of *a, b* and *c*-axis increase linearly with increasing Eu content (*x*).

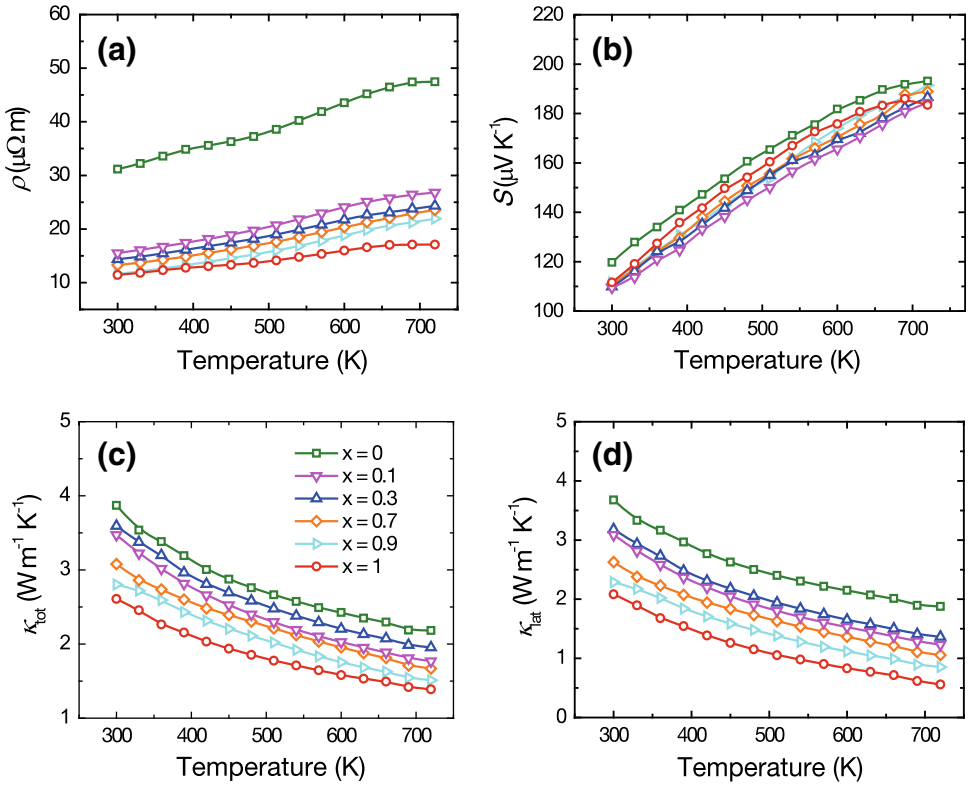

Fig. 3. The temperature dependence of $Ca_{1-x}Eu_xZn_2Sb_2$ samples. (a) electrical resistivity (ρ), (b) Seebeck coefficient (S), (c) total thermal conductivity(κ_{tot}) and (d) lattice thermal conductivity (κ_{lat}).

Table I. The room temperature carrier concentrations (n), carrier motilities (μ_H), Seebeck coefficients (S), electrical resistivity (ρ), and calculated carrier effective mass m^*/m_0 of the $Ca_{1-x}Eu_xZn_2Sb_2$ samples

Nominal composition	n (10^{19}cm^{-3})	μ_H (cm^{2}V^{-1}s^{-1})	S (μV K^{-1})	ρ($\mu\Omega$ m)	m^*/m_0
$CaZn_2Sb_2$	3.04	63.6	119.7	31.2	0.58
$Ca_{0.9}Eu_{0.1}Zn_2Sb_2$	3.29	117.4	111.7	15.5	0.57
$Ca_{0.7}Eu_{0.3}Zn_2Sb_2$	3.59	120.8	109.9	14.4	0.59
$Ca_{0.3}Eu_{0.7}Zn_2Sb_2$	3.81	123.6	111.0	13.3	0.62
$Ca_{0.1}Eu_{0.9}Zn_2Sb_2$	3.83	140.0	111.7	11.6	0.63
$EuZn_2Sb_2$	2.94	186.2	111.6	11.5	0.52

Which is obtained by Reitveld refinement method. This result is in agreement with Vegard's law. As shown in Fig. 2b, the lattice parameters of $EuZn_2Sb_2$ are larger than that of $CaZn_2Sb_2$, and this trend agrees with atomic sizes.[18–20] All of these findings give a reasonable indication that Eu atoms successfully occupy Ca sites in $CaZn_2Sb_2$.

Figure 3 shows the temperature dependence of electrical and thermal transport properties of the samples in the 300–720 K. As shown in Fig. 3a, the electrical resistivity ρ of all samples increase with increasing temperature, indicating the transport property of a semi-metal or degenerate semiconductor. Similar trends were also observed in $Ca_xYb_{1-x}Zn_2Sb_2$, AZn_2Sb_2 (A = Sr, Ca, Yb, Eu) and $EuZn_2Sb_2$ crystals.[9,15,21] It also shows that ρ can be greatly reduced by Eu substitution. Recent study of a single crystal AZn_2Sb_2(Ca, Eu, Yb) phase clearly shown that larger carrier mobility of rare-earth related compounds appears to be an inherent features of these materials, and is not related to sample purity.[19] This confirms that larger zT is found in Eu doped samples due to higher carrier mobility. In addition, the carrier concentration slightly increases with increasing Eu content. This result is similar to that of reported polycrystalline and single crystal samples[15,16,19,21] but with a small difference. This small difference may be due to the presence of unavoidable trace amount of impurity phases in $Ca_{1-x}Eu_xZn_2Sb_2$ samples. Meanwhile, the carrier mobility of Eu-substituted samples upsurges about twofold compared to that of pristine

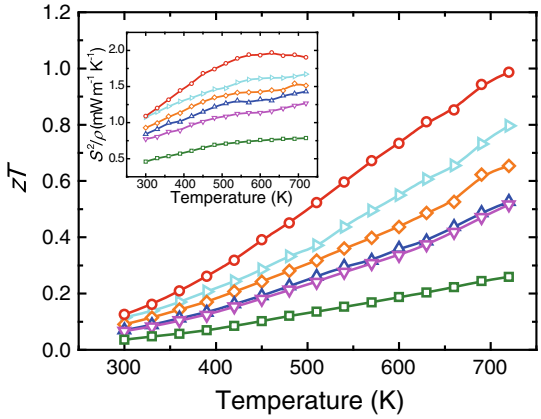

Fig. 4. Temperature dependence of thermoelectric figure of merit zT and the inset shows the power factor of $Ca_{1-x}Eu_xZn_2Sb_2$ ($0 \le x \le 1$) samples.

$CaZn_2Sb_2$. Since $1/\rho = ne\mu$, the increase in carrier mobility leads to the significant reduction in electrical resistivity.

Figure 3b shows the temperature dependence of Seebeck coefficient S for the series of compounds. The Seebeck coefficient rises almost linearly as the temperature increases, which is analogues to previously reported data.[9,15] Surprisingly, the S curves of all Eu-substituted samples are almost invariant when electrical resistivity ρ decreases. They are slightly lower than that of $CaZn_2Sb_2$ by 10%. For metals or degenerate semiconductors, with the assumption of parabolic band and energy independent scattering,[22,23] the Seebeck coefficient is proportional to T and $n^{-2/3}$ according to Eq. 1.

$$S = \frac{8\pi^2 K_B^2 T}{3eh^2} m^* \left(\frac{\pi}{3n}\right)^{\frac{2}{3}} \quad (1)$$

where n is a carrier concentration, e is the charge of an electron, h is plank's constant, m^* is the effective mass and k_B is Boltzmann's constant. This relation gives $m^* = (0.59 \pm 0.03)\, m_0$ for all x (Table I). The low effective mass, relatively high mobility and high Seebeck coefficient indicate the band semiconductor behavior as opposed to the bipolar conduction.[9]

Figure 3c gives the temperature dependence of the total thermal conductivity κ. It is the contribution of phonon (lattice part κ_L) and charge carriers (electronic part κ_e). The total thermal conductivity decreases with increasing Eu content(x). Furthermore, the lattice thermal conductivity is significantly reduced which could be ascribed to enhancement of phonon scattering by dopants with greater atomic weight. For all the series of $Ca_{1-x}Eu_xZn_2Sb_2$ the κ value decreases dramatically with increasing temperature. As shown in Fig. 3d, the lattice thermal conductivity monotonically decreases as the Europium content (x) increases. The lattice thermal conductivity κ_{Lat} of each series is calculated by subtracting electronic thermal conductivity κ_e from total thermal conductivity κ. The κ_e can be evaluated from Wiedemann–Franz relation $\kappa_e = LT\sigma$, where L is 2.45×10^{-8}W Ω K^{-2}, σ is the electrical conductivity, and T is the corresponding absolute temperature. The κ value of $EuZn_2Sb_2$ and Eu substituted samples are lower than $CaZn_2Sb_2$, which is in agreement with rare-earth derived compounds reported in the literature.[9,15]

Since the Eu-substituted samples exhibit lower electrical resistivity, they would possess much higher power factor. The power factors S^2/ρ of all the samples were calculated and indicated in the inset of Fig. 4. It shows that the S^2/ρ curve rises with increasing Eu content and it achieves 1.93 mW m^{-1} K^{-2} at 690 K for $EuZn_2Sb_2$, which is about three times higher than $CaZn_2Sb_2$. The higher power factor arises from the lower electrical resistivity, which are typically associated with a large carrier mobility and an optimal carrier concentration, while the Seebeck coefficient is almost invariant.

The temperature dependence of zT curves for $Ca_{1-x}Eu_xZn_2Sb_2$ are calculated from the measured value of ρ, S, and κ as shown in Fig. 4. All the Eu-substituted samples show comparable zT in the temperature range measured from 300 K to 720 K. It is noticed that the zT values increase when $CaZn_2Sb_2$ is doped with Eu that means small amount of Eu could significantly enhance the thermoelectric performance of $CaZn_2Sb_2$. The zT value of heavily doped $Ca_{0.1}Eu_{0.9}Zn_2Sb_2$ achieved 0.8 at 720 K. Meanwhile, the highest zT value was observed in $EuZn_2Sb_2$, consistent with previously reported literature data[21] which was about 0.98 and $CaZn_2Sb_2$ achieved zT value of about 0.26 at 720 K.

CONCLUSION

In summary, we investigated the thermoelectric favorable transport properties of $Ca_{1-x}Eu_xZn_2Sb_2$ ($0 \le x \le 1$) Zintl phase compounds. Tuning the electrical and thermal transport property could be a powerful method to achieve a larger zT. Thus, the carrier mobility of all Eu-substituted samples increase about twofold higher than the pristine $CaZn_2Sb_2$. As a result the electrical resistivity decreases significantly. The power factor increases remarkably because of the decreasing electrical resistivity but almost invariant Seebeck coefficient. Furthermore, this favorable thermoelectric performance originated from reduction of thermal conductivity due to phonon scattering by the rare earth element Eu and substantial increment of electrical conductivity. Consequently, cationic substitution of rare earth element significantly increased the thermoelectric dimensionless figure of merit for all Europium substituted samples.

ACKNOWLEDGEMENTS

The authors would like to thank Chia-Hsiang Chang for technical help. This work is financially supported by Academia Sinica and Ministry of Science and Technology (MOST), Taiwan, Grant No. MOST 103-2112-M-001-021-MY3.

REFERENCES

1. S. Kim, K.H. Lee, H.A. Mun, H.S. Kim, S.W. Hwang, J.W. Roh, D.J. Yang, W.H. Shin, X.S. Li, Y.H. Lee, G.J. Snyder, and S.W. Kim, *Science* 348, 109 (2015).
2. L.D. Zhao, S.H. Lo, Y. Zhang, H. Sun, G. Tan, C. Uher, C. Wolverton, V.P. Dravid, and M.G. Kanatzidis, *Nature* 508, 373 (2014).
3. L.D. Zhao, V.P. Dravid, and M.D. Kanatzidis, *Energy Environ. Sci.* 7, 251 (2014).
4. T.M. Tritt and M.A. Subramanian, *MRS Bull.* 31, 188 (2006).
5. G.J. Snyder and E.S. Toberer, *Nat. Mater.* 7, 105 (2008).
6. S.M. Kauzlarich, S.R. Brown, and G.J. Snyder, *Dalton Trans.* 21, 2099 (2007).
7. E.S. Toberer, A.F. May, and G.J. Snyder, *Chem. Mater.* 22, 624 (2010).
8. C. Yu, T.J. Zhu, S.N. Zhang, X.B. Zhao, J. He, Z. Su, and T.M. Tritt, *J. Appl. Phys.* 104, 013705 (2008).
9. F. Gascoin, S. Ottensmann, D. Stark, S.M. Haile, and G.J. Snyder, *Adv. Funct. Mater.* 15, 1860 (2005).
10. S.R. Brown, S.M. Kauzlarich, F. Gascoin, and G.J. Snyder, *Chem. Mater.* 18, 1873 (2006).
11. X.J. Wang, M.B. Tang, H.H. Chen, X.X. Yang, J.T. Zhao, U. Burkhardt, and Y. Grin, *Appl. Phys. Lett.* 94, 092106 (2009).
12. H. Zhang, M.B. Tang, W. Schnelle, M. Baitinger, Z.Y. Man, H.H. Chen, X.X. Yang, J.T. Zhao, and Y. Grin, *J. Electron. Mater.* 39, 9 (2010).
13. A. Zevalkink, W.G. Zeier, G. Pomrehn, E. Schechtel, W. Tremel, and G.J. Snyder, *Energy Environ. Sci.* 5, 9121 (2012).
14. A. Zevalkink, Y. Takagiwa, K. Kitahara, K. Kimura, and G.J. Snyder, *Dalton Trans.* 43, 4720 (2014).
15. E.S. Toberer, A.F. May, B.C. Melot, E.F. Larsen, and G.J. Snyder, *Dalton Trans.* 39, 1046 (2010).
16. G. J. Snyder and D. Stark, *21st International conference on thermoelectric* (Long Beach, CA, USA, 2002).
17. G. Kai, C. Qigao, and Z. Jingtai, *J. Rare Earths* 31, 11 (2013).
18. C.A. Uvarov, F.O. Alvarez, and S.M. Kauzlarich, *Inorg. Chem.* 51, 7617 (2012).
19. Andrew F. May, Michael A. McGuire, Jie Ma, Olivier Delaire, Ashfia Huq, and Radu Custelcean, *J. Appl. Phys.* 111, 033708 (2012).
20. R.D. Shannon, *Acta Cryst.* A32, 751 (1976).
21. H. Zhang, J.T. Zhao, Yu Grin, X.J. Wang, M.B. Tang, Z.Y. Man, H.H. Chen, and X.X. Yang, *J. Chem. Phys.* 129, 164713 (2008).
22. M. Culter, J.F. Leavy, and R.L. Fitzpatrick, *Phys. Rev.* 133, A1143 (1964).
23. B.K. Min, B.S. Kim, I.H. Kim, J.K. Lee, M.H. Kim, M.W. Oh, S.D. Park, and H.W. Lee, *Electron. Mater. Lett.* 7, 255 (2011).